

Dynamic analysis of major public health emergency transmission considering the dual-layer coupling of community-resident complex networks

Peng Yang(杨鹏), Ruguo Fan(范如国), Yibo Wang(王奕博), and Yingqing Zhang(张应青)

Citation: Chin. Phys. B, 2024, 33 (**7**): 070206. DOI: 10.1088/1674-1056/ad39c7
Journal homepage: http://cpb.iphy.ac.cn; http://iopscience.iop.org/cpb

What follows is a list of articles you may be interested in

Prediction of collapse process and tipping points for mutualistic and competitive networks with *k*-core method

Dongli Duan(段东立), Feifei Bi(毕菲菲), Sifan Li(李思凡), Chengxing Wu(吴成星), Changchun Lv(吕长春), and Zhiqiang Cai(蔡志强)
Chin. Phys. B, 2024, 33 (**5**): 050201. DOI: 10.1088/1674-1056/ad3341

Intervention against information diffusion in static and temporal coupling networks

Yun Chai(柴允), You-Guo Wang(王友国), Jun Yan(颜俊), and Xian-Li Sun(孙先莉)
Chin. Phys. B, 2023, 32 (**9**): 090202. DOI: 10.1088/1674-1056/acb9f4

Robustness measurement of scale-free networks based on motif entropy

Yun-Yun Yang(杨云云), Biao Feng(冯彪), Liao Zhang(张辽), Shu-Hong Xue(薛舒红), Xin-Lin Xie(谢新林), and Jian-Rong Wang(王建荣)
Chin. Phys. B, 2022, 31 (**8**): 080201. DOI: 10.1088/1674-1056/ac6942

Effect of observation time on source identification of diffusion in complex networks

Chaoyi Shi(史朝义), Qi Zhang(张琦), and Tianguang Chu(楚天广)
Chin. Phys. B, 2022, 31 (**7**): 070203. DOI: 10.1088/1674-1056/ac5985

Dynamics and intermittent stochastic stabilization of a rumor spreading model with guidance mechanism in heterogeneous network

Xiaojing Zhong(钟晓静), Yukun Yang(杨宇琨), Runqing Miao(苗润青), Yuqing Peng(彭雨晴), and Guiyun Liu(刘贵云)
Chin. Phys. B, 2022, 31 (**4**): 040205. DOI: 10.1088/1674-1056/ac587d

---

Dynamic analysis of major public health emergency transmission considering the dual-layer coupling of community–resident complex networks

Peng Yang(杨鹏)[1], Ruguo Fan(范如国)[1], Yibo Wang(王奕博)[2,†], and Yingqing Zhang(张应青)[3]

[1] *School of Economics and Management, Wuhan University, Wuhan* 430072, *China*
[2] *Postdoctoral Research Station, China International Engineering Consulting Corporation, Beijing* 100000, *China*
[3] *School of Business Administration, Guizhou University of Finance and Economics, Guiyang* 550025, *China*

(Received 4 December 2023; revised manuscript received 5 March 2024; accepted manuscript online 3 April 2024)

We construct a dual-layer coupled complex network of communities and residents to represent the interconnected risk transmission network between communities and the disease transmission network among residents. It characterizes the process of infectious disease transmission among residents between communities through the SE2IHR model considering two types of infectors. By depicting a more fine-grained social structure and combining further simulation experiments, the study validates the crucial role of various prevention and control measures implemented by communities as primary executors in controlling the epidemic. Research shows that the geographical boundaries of communities and the social interaction patterns of residents have a significant impact on the spread of the epidemic, where early detection, isolation and treatment strategies at community level are essential for controlling the spread of the epidemic. In addition, the study explores the collaborative governance model and institutional advantages of communities and residents in epidemic prevention and control.

Keywords: propagation dynamics, complex networks, public health events, community structure

PACS: 02.70.–c, 02.60.–x **DOI:** 10.1088/1674-1056/ad39c7

1. Introduction

The COVID-19 pandemic has affected the lives of billions, significantly impacting health, economy, environment and social sectors, plunging the global economy into its most severe recession since World War II.[1] This crisis has underscored the crucial role of public health systems in controlling infectious diseases, revealing inadequacies in current systems. This demands not only enhanced governance and intervention efficacy from nations but also necessitates in-depth research into the mechanisms of pandemic spread to better handle future crises.

Looking at China's early COVID-19 containment experience, community-level control proved effective in slowing the spread, buying time for medical institutions.[2] Communities, defined as social collectives within specific geographic areas,[3] form the basic units of grassroots governance in China, with clear institutional identities, geographic boundaries, populations and dedicated service personnel. Due to the covert nature of infectious diseases and the characteristics of community transmission, communities have become significant transmission spaces, making community-level control a key link in halting the spread of the pandemic.[4–6] Before effective drugs for treating infectious diseases are developed, early detection, isolation and treatment are effective methods to control the spread.[7,8] Therefore, understanding the impact of community structures and resident relationships on the spread, and quantifying the role of community control mechanisms in pandemic prevention are the focus of this study.

The SEIR model, a classic compartmental model in transmission dynamics,[9] considers the significant incubation period of infectious diseases, using a latent state compartment as a transition from susceptible to infected states. Many studies have validated its effectiveness in depicting the transmission mechanisms of latent period diseases in real-world societies.[10,11] Building on this, the SEIHR model was proposed,[12] introducing a new compartment H for hospitalized individuals, which allows analysis of the speed at which infections are diagnosed and admitted, and the interaction with other compartments post-admission, affecting disease spread. Researchers have expanded on this for diseases such as Ebola, MERS and COVID-19, achieving valuable results in transmission analysis, prevention strategy effectiveness and basic reproduction number calculations.[13–17]

Research based on compartmental models typically assumes uniform mixing networks, overlooking the impact of local contacts on disease spread, a premise inconsistent with reality.[18,19] The evolution of complex network science offers new perspectives and approaches for studying pandemic transmission mechanisms. As scholars delved deeper, Watts and Strogatz's discovery of small-world properties in human contact patterns revealed that different network types affect disease spread speed and range — diseases spread

[†]Corresponding author. E-mail: yibowong@qq.com

© 2024 Chinese Physical Society and IOP Publishing Ltd

faster and wider in small-world networks compared to regular networks.[20] Researchers are increasingly studying transmission mechanisms on complex network levels, with Hsu *et al.*[21] considering the impact of air travel in their mathematical modeling of H5N1 and H1N1 influenza, analyzing the effect of passenger behavior in small-world networks and the potential efficacy of airport control measures. Li *et al.*[22] developed a small-world network-based model considering incubation periods and asymptomatic carriers to describe COVID-19 spread, assessing the effectiveness of different prevention measures at various stages. Thurner *et al.*[23] proposed a network-structured model akin to SIR to explain the linear growth in infection rates, a phenomenon with which traditional compartment models struggle, finding that this approach naturally explains the occurrence of linear growth rates. Furthermore, they discovered that this model can accurately describe the impact of non-pharmaceutical interventions on epidemic spread without the need for parameter fitting and tuning. Researchers have found that combining compartmental transmission models with complex network structures better describes the impact of human behavior on epidemic spread.[24,25]

Integrating compartment models with two-tier or multi-tier complex networks for the study of information and disease propagation has become a new trend in recent years. In particular, the interaction mechanism between information dissemination and disease spread is of paramount importance. Researchers, such as He and Zhu,[26] Zhao *et al*,[27] Li *et al.*[28] and Ma *et al*.[29] have proposed dual-layer or multi-layer network models that combine the viral transmission layer with the information dissemination layer. These models are utilized to simulate the interactive spread of viruses and related awareness. Studies indicate that spreading positive information, increasing media coverage and enhancing the rate of awareness dissemination can effectively prevent the spread of epidemics. This is closely related to the interaction between the epidemic and the information dissemination layer. Another significant research direction is exploring the impact of different social relationships on disease transmission. Scabini *et al*,[30] Chung and Chew,[31] and Turker and Bingol[32] developed network models encompassing multiple facets such as household, workplace, school, and friendship layers to observe the influence of different social activity layers on disease transmission rates. The findings suggest that prioritizing the management of the "friendship" layer can significantly slow down the spread of epidemics, providing valuable insight and effective measures for understanding and controlling pandemics. However, theoretical research on disease transmission models with community structures and preventive measures such as increasing social distancing and implementing community quarantines remains insufficient,[33] necessitating further exploration.

The impact of community structures and resident relationships on epidemic spread, and quantifying the role of communities in pandemic control are central to this study. Existing literature predominantly focuses on the transmission process, exploring various transmission characteristics and dynamical mechanisms, with scant attention to the influence of real-world social structures on transmission. However, in real life, a community is a social living community with spatial boundaries, tied together by geographical or residential relationships, and residents' relational networks are somewhat constrained by their community affiliations.[34]

In this paper, the definition of public health risks references the related reports by the World Health Organization (WHO),[35] where "health risks" are defined as factors that increase the probability of adverse health outcomes. Particularly during the Covid-19 pandemic, scholars have connected the concept of "health risks" with the spread and impact of Covid-19, examining how health risks manifest geographically during the pandemic and how urban and regional planning can address these risks.[36] Thus, we adopt these perspectives, considering "health risks" as various risk factors related to health, such as disease transmission, environmental pollution, unsafe food and water sources, especially in the context of sudden public health events such as infectious disease outbreaks or environmental disasters, posing threats to public health.

In this paper, we have developed the SE2IHR transmission dynamics model that considers two different types of outlier infectors and diagnosed and treated patients, to characterize the transmission mechanism of public health risk events. Classic compartment models can be seen as transmission unfolding in uniformly mixed, fully connected networks. These models are simple and facilitate fitting and analysis, effectively reflecting the true trend of epidemic spread. However, when aiming to further analyze the impact of social structures and control measures on epidemic spread, these models lack finer-grained depictions of social structures. Therefore, to study the influence of real-world community structures and community-level control mechanisms on epidemic spread, we consider the social network structures formed among residents and the coupling between community–resident complex networks. This dual approach enables us to study the impact of complex network structures on epidemic diffusion while also validating through further simulation experiments the critical role of community control in pandemic prevention.

2. Propagation model incorporating the dual-layer coupling of community–resident networks

To further explore the impact of community structures and various prevention measures on controlling the spread of significant public health emergencies, in this section we

construct a dual-layer complex network representing the inter-community risk transmission network and the intra-community disease transmission network among residents. The structure of this model is illustrated in Fig. 1. Nodes in different layers of the network represent different entities. In the community layer, each node represents a community, while in the resident layer, each node represents an individual resident. The connections between nodes at different levels have different meanings, which are detailed in Subsections 2.1 and 2.2. Risk events are transmitted between adjacent nodes in the community network layer, while the epidemic spreads within the social network layer of residents. Assuming there are $N_{\text{Community}}$ nodes in the community network layer, and each community consists of a network of N_{Resident} nodes due to the subordinate relationship between communities and their residents.

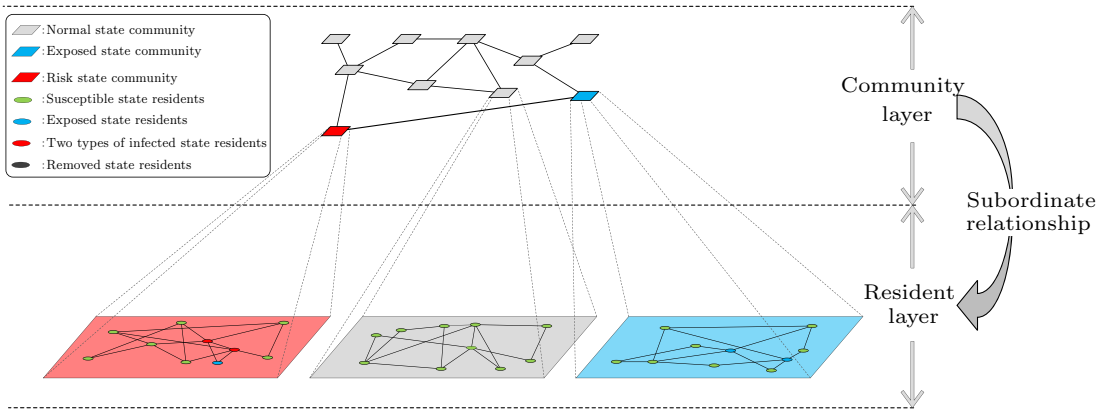


Fig. 1. The dual-layer coupling of community–resident networks.

2.1. Resident layer: SE2IHR network model with two types of infectors

For the resident layer, this study proposes the SE2IHR model based on complex network theory, considering six different groups: susceptible (S), exposed (E), type 1 infection (I_1), type 2 infection (I_2), hospitalized (H), removed (R). This model more intricately defines the states and transmission dynamics of different types of infected populations, dividing the unadmitted infected group into two independent compartments: type 1 infection (unadmitted infectors) and type 2 infection (to-be-admitted infectors). Addressing the long incubation periods characteristic of some infectious diseases, this paper follows other researchers' methods[10,11,37] by setting a latent state compartment to simulate the condition of patients during the incubation period.

Considering the transmission characteristics of significant public health emergencies, this paper provides definitions for each group in the SE2IHR model (the dynamical transmission characteristics of the model are shown in Fig. 2).

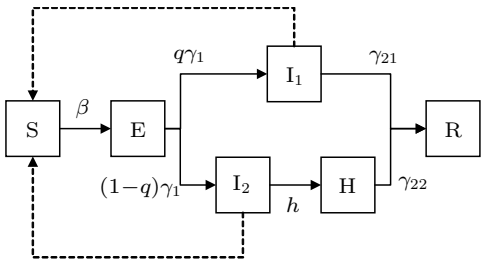


Fig. 2. Dynamical transitions in the SE2IHR model.

Susceptible group (S): the susceptible group represents the potential population at risk of infection. Individuals are susceptible before being infected, meaning they can be infected by an infectious person with whom they come into contact. After contact with an infector, susceptible individuals transition to the exposed group with a certain probability.

Exposed group (E): due to the significant incubation period characteristic of some diseases, the exposed group represents those who have been infected after contact with an infector but are still asymptomatic and in the incubation period. After a certain incubation period, exposed individuals transition to one of the two infection groups with a certain probability. It is generally assumed that the exposed group lacks the ability to transmit the infection.

Type 1 infection group (I_1): this group represents individuals who have shown symptoms of infection and can transmit the disease. Type 1 infectors are those who have not been detected and diagnosed by medical institutions throughout their infection period, either due to personal reasons or limited detection and treatment capacity of medical institutions. They remain undetected within the population but are still contagious. After a period of illness, these infectors transition to the removed group. The type 1 infected individuals (I_1) can be regarded as asymptomatic carriers, which is consistent with most existing disease transmission models. That is, a proportion q of asymptomatic carriers in all infected individuals, as seen in clinical statistics, is used to reflect the infection status of the first class of infected individuals (I_1).

Type 2 infection group (I_2): in contrast with type 1, type 2 infectors are those who will be detected, diagnosed and treated by medical institutions but have not yet been diagnosed. This

group also has the capability to transmit the disease and transitions to the hospitalized group with a certain probability. The type 2 infected individuals (I_2) can be considered as the precursor state to the confirmed treatment status (H), which is exactly the number of cases observable in various statistical data. Thus, the second class of infected individuals (I_2) can be estimated based on the daily number of newly treated cases and the probability h of being treated per unit of time. Their transition speed depends on local medical conditions and the level of resources available.

Hospitalized group (H): this group consists of patients who have been diagnosed through clinical diagnosis or nucleic acid testing and are receiving treatment. Often placed in isolation wards and treated by medical workers wearing protective gear, it is assumed in this study that the hospitalized group is not infectious.

Removed group (R): this group includes individuals who have gone through the entire disease cycle and are no longer affected by the infectious disease, typically those who have recovered or died.

Furthermore, this paper considers the heterogeneity of resident contact patterns and the structure of social networks on epidemic transmission, proposing a resident-level epidemic transmission network model. Intra-community social networks among residents are relatively fixed, with overlapping residential and living paths. Connections between resident nodes indicate stable contacts and close social distances. The resident-level network has a total of $N_{\text{Community}} \times N_{\text{Resident}}$ nodes, with $N_{\text{Community}}$ parallel sub-networks representing each community and N_{Resident} nodes in each sub-network representing the total number of residents within each community's jurisdiction.

We first analyze the transmission mechanism within a single sub-network. The node states are set as follows: susceptible (S), exposed (E), type 1 infection (I_1), type 2 infection (I_2), hospitalized (H), removed (R). Within each time step, the epidemic spreads from infected nodes (I_1, I_2) to adjacent susceptible nodes with a probability β_r through the network edges. Susceptible nodes exposed to infected ones go through an incubation (E) period before becoming infected. Exposed residents transition to type 1 infection with probability $q\gamma_1$ and to type 2 infection with probability $(1-q)\gamma_1$ at each time step. Meanwhile, type 1 infectors transition to the removed group with probability γ_{21}, type 2 infectors are diagnosed and treated with probability h, and hospitalized patients transition to the removed group with probability γ_{22}. Let n_r be the maximum degree k_r of nodes in the resident network. $P_{k_r}(k_r = 1,2,\ldots,n_r)$ is the proportion of nodes with degree k_r among all nodes, meaning $P_{k_r} = 0$ for $k_r > n_r$. Let $S_{k_r}(t)$, $E_{k_r}(t)$, $I_{1,k_r}(t)$, $I_{2,k_r}(t)$, $H_{k_r}(t)$ and $R_{k_r}(t)$ respectively represent the number of resident nodes at time t with node degree k_r in each state. This paper considers two categories of active infectors and hospitalized patients at the resident level, establishing the SE2IHR model on a complex network as follows:

$$\begin{aligned}
\frac{\mathrm{d}S_{k_r}(t)}{\mathrm{d}t} &= -\beta_r k_r S_{k_r}(t)[\Theta_1(t)+\Theta_2(t)],\\
\frac{\mathrm{d}E_{k_r}(t)}{\mathrm{d}t} &= \beta_r k_r S_{k_r}(t)[\Theta_1(t)+\Theta_2(t)] - \gamma_{1,r}E_{k_r}(t),\\
\frac{\mathrm{d}I_{1,k_r}(t)}{\mathrm{d}t} &= q\gamma_{1,r}E_{k_r}(t) - \gamma_{21}I_{1,k_r}(t),\\
\frac{\mathrm{d}I_{2,k_r}(t)}{\mathrm{d}t} &= (1-q)\,\gamma_{1,r}E_{k_r}(t) - hI_{2,k_r}(t),\\
\frac{\mathrm{d}H_{k_r}(t)}{\mathrm{d}t} &= -hI_{2,k_r}(t) - \gamma_{22}H_{k_r}(t),\\
\frac{\mathrm{d}R_{k_r}(t)}{\mathrm{d}t} &= \gamma_{21}I_{1,k_r}(t) + \gamma_{22}H_{k_r}(t).
\end{aligned} \tag{1}$$

In this context, $\Theta_1(t)$ represents the probability of any resident node being connected to a type 1 infection node (I_1), and $\Theta_2(t)$ represents the probability of any resident node being adjacent to a type 2 infection node (I_2). The edges between nodes in the network signify relatively stable social relationships or close physical distances among residents, resulting in stable close contacts. However, even stable close contacts do not guarantee transmission from the two types of infected patients, so we define β_r as the effective transmission rate. N_{Resident} is the number of residents in each community's jurisdiction, and N_{k_r} is the number of nodes with degree k_r, so $\sum_{k_r=1}^{n} N_{k_r} = N_{\text{Resident}}$,

$$\begin{aligned}
N_{k_r} \;=\; & S_{k_r}(t) + E_{k_r}(t) + I_{1,k_r}(t)\\
& + I_{2,k_r}(t) + H_{k_r}(t) + R_{k_r}(t),\\
& (k_r = 1,2,\ldots,n_r).
\end{aligned} \tag{2}$$

We assume that once the network structure is generated, it does not change; that is, each sub-network's degree distribution is fixed. Based on this definition, we can express the probability of any node being connected to the two types of infection nodes:

$$\Theta_1(t) = \frac{1}{\overline{k}_r}\sum_{k_r=1}^{n} k_r P_{k_r}\frac{I_{1,k_r}(t)}{N_{\text{Resident},k_r}}, \tag{3}$$

$$\Theta_2(t) = \frac{1}{\overline{k}_r}\sum_{k_r=1}^{n} k_r P_{k_r}\frac{I_{2,k_r}(t)}{N_{\text{Resident},k_r}}. \tag{4}$$

Considering realistic constraints, we provide the constraint conditions:

$$\begin{cases}
S_{k_r}(t) + E_{k_r}(t) + I_{1,k_r}(t) + I_{2,k_r}(t) + H_{k_r}(t) + R_{k_r}(t) = N_{k_r},\\
0 \le S_{k_r}(t),\ E_{k_r}(t),\ I_{1,k_r}(t),\ I_{2,k_r}(t),\ H_{k_r}(t),\ R_{k_r}(t) \le N_{k_r}.
\end{cases} \tag{5}$$

The basic reproduction number is a crucial indicator for measuring the transmission capability of an infectious disease. It generally refers to the average number of other individuals that the initial case of an infection can infect under conditions where there is no intervention, control measures are absent, and all individuals are susceptible to infection at the onset of an outbreak.[38] In this section, we refer to the research methods of Diekmann *et al.*,[39] Guerra *et al.*[40] and Mwalili *et al.*[41] to derive the basic reproduction number of the SE2IHR infectious disease model proposed in this paper using the next-generation matrix method. The largest eigenvalue or spectral radius of the next-generation matrix is defined as the basic reproduction number.

The infectious disease model proposed in this paper divides the population into six different compartments based on the different stages of infection status individuals are in. Therefore, in this paper, we define $X=(x_1,x_2,x_3,x_4,x_5,x_6)$ as the combination of various compartments, which represents the number of individuals in each compartment. The matrix represents the rate of increase of individuals in each compartment, with $J(x)$ being the vector of $j_i(x)$. Similarly, it is defined as the rate of removal of individuals from each compartment, with $V(x)$ being the vector of $v_i(x)$. Based on the differential equations of the SE2IHR infectious disease model, expressions can be obtained as

$$J(X)=\begin{bmatrix}\beta_r\overline{k_r}S_{k_r}(t)(I_{1,k_r}(t)+I_{2,k_r}(t))\\0\\0\\0\\0\\0\end{bmatrix}, \tag{6}$$

$$V(X)=\begin{bmatrix}\gamma_1 E_{k_r}(t)\\ \beta_r\overline{k_r}S_{k_r}(t)(I_{1,k_r}(t)+I_{2,k_r}(t))\\ \gamma_{21}I_{1,k_r}(t)-q\gamma_{1,r}E_{k_r}(t)\\ hI_{2,k_r}(t)-(1-q)\gamma_{1,r}E_{k_r}(t)\\ \gamma_{22}H_{k_r}(t)-hI_{2,k_r}(t)\\ -\gamma_{21}I_{1,k_r}(t)-\gamma_{22}H_{k_r}(t)\end{bmatrix}. \tag{7}$$

Subsequently, we define $\boldsymbol{J}$ and $\boldsymbol{V}$ as the Jacobian matrices of $J(X)$ and $V(X)$, respectively. Thus, the Jacobian matrix concerning X can be obtained by

$$\boldsymbol{J}=\begin{bmatrix}F&0\\0&0\end{bmatrix},\quad \boldsymbol{V}=\begin{bmatrix}V&0\\J_3&J_4\end{bmatrix}. \tag{8}$$

From this, we can construct the matrices F and V, here considering only the states E, I_1, and I_2, as these states are directly related to new infections and state transitions. The expressions for F and V can be obtained as

$$F(X)=\begin{bmatrix}0&\beta\overline{k_r}&\beta\overline{k_r}\\0&0&0\\0&0&0\end{bmatrix},$$

$$V(X)=\begin{bmatrix}\gamma_{1,r}&0&0\\-q\gamma_{1,r}&\gamma_{21}&0\\-(1-q)\gamma_{1,r}&0&h\end{bmatrix}. \tag{9}$$

Therefore, the next-generation matrix of the system is defined as follows:

$$\begin{aligned}FV^{-1}&=\begin{bmatrix}0&\beta\overline{k_r}&\beta\overline{k_r}\\0&0&0\\0&0&0\end{bmatrix}\times\begin{bmatrix}\frac{1}{\gamma_{1,r}}&0&0\\\frac{q}{\gamma_{21}}&\frac{1}{\gamma_{21}}&0\\\frac{1-q}{h}&0&\frac{1}{h}\end{bmatrix}\\&=\begin{bmatrix}\frac{\beta\overline{k_r}(hq-q\gamma_{21}+\gamma_{21})}{h\gamma_{21}}&\frac{\beta\overline{k_r}}{\gamma_{21}}&\frac{\beta\overline{k_r}}{h}\\0&0&0\\0&0&0\end{bmatrix}.\end{aligned} \tag{10}$$

The largest eigenvalue or spectral radius of the next-generation matrix is defined as the basic reproduction number

$$R_0=\frac{\beta\overline{k_r}(hq-q\gamma_{21}+\gamma_{21})}{h\gamma_{21}}. \tag{11}$$

2.2. Community layer: Community-associated risk transmission network model

At the community layer, we propose the NERN (normal–exposed–risk–normal) model based on the SEIS model mechanism[42] in complex networks, with the network transmission dynamics illustrated in Fig. 3. In our community network layer, edges between nodes represent geographical proximity between different communities. When sudden public health events occur, health risks are more likely to spread between geographically close communities. Residents of different communities located close to each other are more likely to have risk contacts in public areas at the community boundaries (such as supermarkets, community clinics, restaurants, etc.). The community layer's network consists of $N_{\text{Community}}$ nodes, and the state of each node is related to the state of all residents in its jurisdiction, which will be elaborated in the following sections.

In our proposed NERN model, R represents the risk state of a community node, meaning the community contains infectious residents (I_1, I_2) and has the capacity to transmit the risk to other communities. E represents the exposed state of a community node. Communities in the risk state can spread the risk to other adjacent communities, but when susceptible residents in normal state communities have risk contact with infected residents in risk state communities, residents do not immediately transition to the infected state due to the incubation period, at which point the community status is set to the exposed state. N represents the normal state of a community node. When there are no infected residents (I_1, I_2) in the community, the community status is set to normal (N).

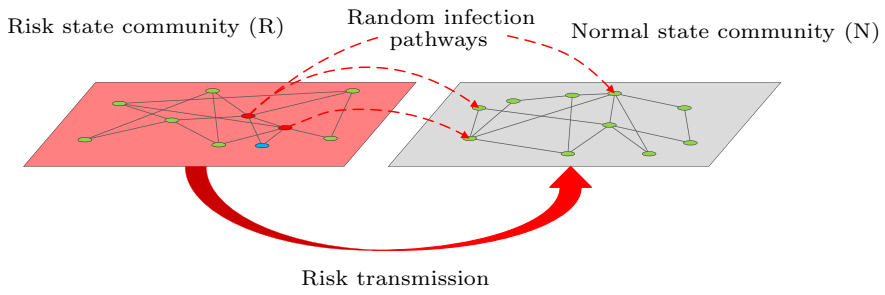


Fig. 3. Schematic diagram of the process of establishing random connecting edges in community risk propagation.

Within each time step, risk events in the community layer propagate from a community node in the risk state (R) to adjacent normal state community nodes (N) with a probability β_c. Given the strong randomness in contacts between residents of neighboring communities in the network, it is assumed that when a normal state community node (N) is influenced by a risk state community node (R), susceptible residents (S) within the normal state community randomly establish connections with infected residents (I_1, I_2) in the risk state community (R) and get infected. Whenever a community in a normal state (N) is infected by a community in a risk state (R), each resident in the risk state community who is in an infected state (I_1, I_2) has a probability of β_r to infect susceptible residents (S) in the normal state community, changing the state of susceptible residents to the exposed state (E). Based on the above mentioned transmission mechanism, we establish the NERN model on a complex network that considers the state of the community as follows:

$$\begin{cases} \dfrac{\mathrm{d}N_{k_c}(t)}{\mathrm{d}t} = -\beta_c k_c N_{k_c}(t)\Theta_c(t) + (\gamma_{1,c}E_{k_c}(t) - \Delta g_{k_c}(t)), \\ \dfrac{\mathrm{d}E_{k_c}(t)}{\mathrm{d}t} = \beta_c k_c N_{k_c}(t)\Theta_c(t) - \gamma_{1,c}E_{k_c}(t), \\ \dfrac{\mathrm{d}R_{k_c}(t)}{\mathrm{d}t} = \Delta g_{k_c}(t), \end{cases} \tag{12}$$

where $\Theta_c(t)$ represents the probability of any normal state community node being adjacent to a risk state community node

$$\Theta_c(t) = \frac{1}{\bar{k}_c}\sum_{k_c=1}^{n} k_c P_{k_c}\frac{R_{k_c}(t)}{N_{\mathrm{Community},k_c}}. \tag{13}$$

$\Delta g_{k_c}(t)$ represents the rate at which risk state communities transition to normal state communities per unit of time. Since the state of the community depends on the status of its residents, we have

$$\Delta g_{k_c}(t) = \sum_{i=1}^{N_{\mathrm{Community}}} g_{k_c,i}(t) - \sum_{i=1}^{N_{\mathrm{Community}}} g_{k_c,i}(t-1), \tag{14}$$

where $g_{k_c,i}(t)$ is an indicator function representing whether each community has both types of infected residents

$$g_{k_c,i}(t) = \begin{cases} 1, \ \sum_{k_r=1}^{n_r} I_{1,k_r}(t) + \sum_{k_r=1}^{n_r} I_{2,k_r}(t) > 0, \\ 0, \ \text{otherwise}. \end{cases} \tag{15}$$

3. Numerical simulation and result analysis

To study the impact of the dual-layer complex network structure of community–residents on disease transmission, in this section, we perform numerical calculations and simulation experiments on the Watts–Strogatz small-world network, using the spreading characteristics of the COVID-19 outbreak as a basis for modeling. Many networks in real life exhibit the structural characteristics of small-world networks, such as social networks,[43] corporate cluster networks,[44] transportation networks[45,46] and community structure networks.[47] Among them, the network generation algorithm that is closely related to community and resident social relationships is the small-world network generation algorithm. This is primarily because interactions in small-world networks feature short average distances and higher clustering coefficients, leading to faster disease transmission speeds, which are more consistent with real-world transmission scenarios.[30] Therefore, considering the balance between data availability and the completeness of the study, we adopt the small-world network generation algorithm as the multi-layer network foundation for the community and resident layers.

The network structure parameters are set based on previous research on social structure networks[48] and physical contact networks between people during the epidemic.[23] In the community network layer, we use a Watts–Strogatz network composed of $N_{\mathrm{Community}} = 100$ nodes, with an average node degree of $\bar{k}_c = 4$ and a random reconnection probability $p_c = 0.2$. Each node in the community network corresponds to a sub-network in the resident layer with $N_{\mathrm{Resident}} = 1000$ nodes, an average node degree of $\bar{k}_r = 3$, and a random reconnection probability $p_r = 0.2$, thus generating $N_{\mathrm{Community}}$ sub-networks of N_{Resident} nodes each in the resident layer.

For the parameters related to infectious disease transmission, the parameters for the resident layer will be set based on the SEIR model, adapted to fit the real COVID-19 data published by the Chinese National Health Commission[49] using the particle swarm optimization algorithm. This approach aims to align the model parameters as closely as possible with the actual public health event. Specifically, the parameters are set as $\beta_r = 0.3$, $\gamma_{1,r} = 0.1923$, $q = 0.1317$, $\gamma_{21} = 0.08$, $\gamma_{22} = 0.1095$, $h = 0.8684$. For the community layer, based on

references[50] and expert recommendations, $\beta_c = 0.1$ is set at 0.1. Simulations are conducted over discrete time steps with a total time $T = 200$. Due to the potential for single experiments to be influenced by randomly generated network structures and random transmission probabilities, multiple repetitions of the experiment are conducted, with the number of repetitions $L = 1000$.

3.1. Numerical simulation of the community–resident dual-layer network model

This section focuses on analyzing the impact of the dual-layer network structure of community–residents on the spread of public health events, without considering the active response measures of the communities. For comparison purposes, we set up a scenario to simulate the absence of community structure, where all residents are in the same network, constructed using the Watts–Strogatz small-world network algorithm with parameters set at ($N'_{\text{Community}} = 1$, $N'_{\text{Resident}} = 100000$), ensuring the total number of residents in the system remains the same. The simulation results for these two cases can be seen in Figs. 3(a)–3(d). We then take $\beta_c = 0.1$ as the baseline case and consider scenarios where community aggregation is sparser ($\beta_c = 0.05$) and denser ($\beta_c = 0.15$), with results shown in Figs. 3(e) and 3(f).

From Figs. 4(a) and 4(b), it can be observed that the trend of the epidemic's development in both single-layer and dual-layer networks is essentially consistent, indicating that the community structure does not affect the transmission characteristics of the infectious disease itself. For example, the peak time for the exposed population precedes the peak time for various infection groups, and the hospitalized group remains the largest infected group in the system.

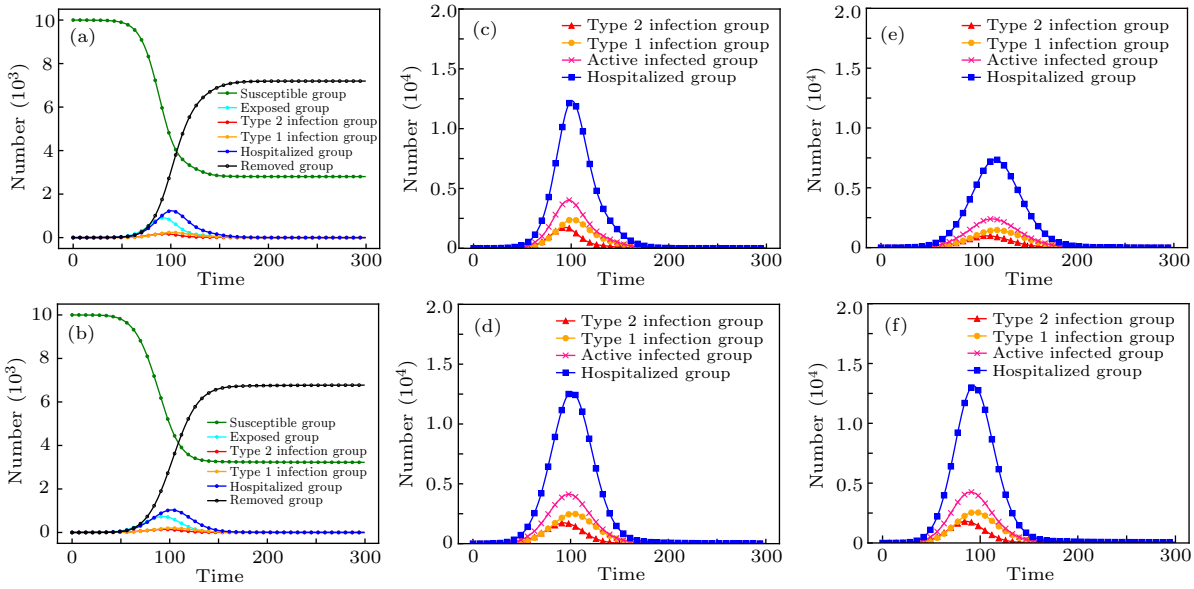


Fig. 4. The impact of community network structure on epidemic spread (a) the development trend of each resident group in a single-layer network, (b) the development trend of each resident group in the presence of a dual-layer community–resident network structure, (c) the development trend of each infection group in a single-layer network, (d) the development trend of each infection group in the presence of a dual-layer community–resident network structure: $\beta_c = 0.1$, (e) the development trend of each infection group in the presence of a dual-layer network structure: $\beta_c = 0.05$, (e) the development trend of each infection group in the presence of a dual-layer network structure: $\beta_c = 0.15$.

Comparing Figs. 4(c) and 4(d), it can be observed that, under baseline conditions, when a community structure is present, the scale of the epidemic's spread (the peak values of first-class infected individuals, second-class infected individuals, and treated individuals) is generally smaller than when there is no community structure. The timing of reaching the peak is largely consistent in both scenarios. However, the rate of increase and decrease of infections is slightly higher when a community structure exists. Further experiments, comparing Figs. 4(d)–4(f), show that when community aggregation is sparser ($\beta_c = 0.05$), the peak values for each infection group are significantly reduced compared to the baseline case ($\beta_c = 0.1$), and the time to reach peak infection is delayed. When community aggregation is denser ($\beta_c = 0.15$), there is no significant change in the peak values for each infection group compared to the baseline case ($\beta_c = 0.1$). The simulation experiments conclude that the community structure impacts the scale and spread speed of the epidemic. Specifically, when there is a community structure, a lower degree of community aggregation implies relatively fewer cross-community–resident risk contacts, meaning the community structure acts as a protective barrier, reducing the peak infection value and slowing the spread of the epidemic. Conversely, when the degree of community aggregation is higher, increased cross-community contacts negate the isolating effect of communities, functioning instead like the long-range links in a small-world network, significantly accelerating the spread of the epidemic.

Observing Fig. 5 further elucidates the harm posed by untraceable cases in the spread of the epidemic. In the early stages of the epidemic, the proportion of new cases transmitted by type 1 infectors (untraceable cases) rapidly rises. As the situation becomes more severe and medical institutions begin to respond, this proportion quickly stabilizes. After the infection rate reaches its peak (as can be seen in Fig. 4(d)), the proportion of new cases transmitted by type 1 infectors gradually increases again. In the later stages of the epidemic, this proportion once again stabilizes but remains at a high level. The simulation results indicate that both in the early and later stages of the epidemic, the transmission ability of type 1 infectors should not be underestimated. Especially in the later stages of the epidemic, sporadically emerging untraceable cases become a major form of epidemic transmission.

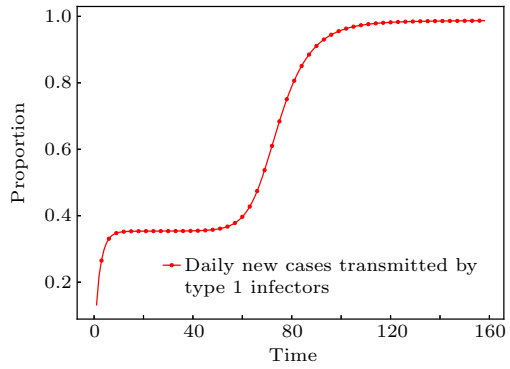


Fig. 5. The proportion of daily new cases transmitted by type 1 infectors.

3.2. Numerical simulation of the community–resident dual-layer network model considering community response measures

In Subsection 3.1, we conducted numerical simulations to analyze epidemic transmission models with and without consideration of community structure. We found that the degree of community aggregation significantly impacts the speed of epidemic spread, highlighting that targeted prevention and control measures at the community level are crucial for controlling the epidemic.

To further investigate the impact of community prevention actions on epidemic spread, we propose the NERCN (normal–exposed–risk–control–normal) model, based on the previously mentioned model. This model incorporates the normal state (N), exposed state (E) and risk state (R) of community nodes, similar to the NERN model. The control state (C) is defined as follows:

When a community node has residents diagnosed and treated (H group), the community's status will switch to the control state.

Simultaneously, if any neighboring community node shifts to the control state due to the presence of diagnosed and treated individuals (H group), that community also transitions to the control state.

A community node in the control state will sever connections with all neighboring nodes (simulating real-life community lockdowns and travel restrictions).

The probability of residents within a community node in the control state getting infected reduces to $\beta_r/2$ (simulating internal community lockdowns, encouraging home isolation and reducing social interaction).

If no newly diagnosed and treated patients (H group) appear within a community node in the control state for 14 consecutive days, it transitions to the normal state.

Based on the description of the control state, we conduct numerical simulations of the community–resident dual-layer network model considering community lockdown measures. The results are shown in Fig. 6.

From Figs. 6(a) and 6(b), it can be observed that after implementing community lockdown measures, the development trend of the epidemic is significantly suppressed compared to the scenario without lockdown measures (as can be seen in Figs. 4(b) and 4(d)). Specifically, the peak number of diagnosed individuals (H group) decreased from 12859 to 148, and the time to reach the peak of the epidemic slowed from $T = 97$ to $T = 63$. Comparing Figs. 6(c) and 6(d), it can be noted that the number of communities affected by the epidemic also significantly decreases when community lockdown measures are implemented. Without lockdown measures, the epidemic freely spreads between communities, quickly affecting all connected communities, as can be seen in Fig. 6(d) where the number of communities in the risk state rapidly rises to a peak and remains at a high level, eventually decreasing as "herd immunity" is formed in the communities. When community lockdown measures are adopted, the communities with diagnosed cases (H group) and their connected communities in the network transition to the control state, maintaining the number of communities that can freely spread risk within the network at a consistently low level. It is noteworthy, according to Figs. 6(e) and 6(f), that the management of associated communities is crucial for the effectiveness of epidemic prevention and control. When no lockdown measures are implemented in communities associated with risk areas, the effectiveness of the lockdown is greatly reduced, the peak number of diagnosed individuals increases, and the fluctuations in the number of risk communities rise. From Fig. 6(b), it can be seen that the number of hospitalized individuals reaches a first peak at $T = 63$ and a second, slightly lower peak at $T = 193$, decreasing from 148 to 61 individuals. The results indicate that community lockdown measures can control the epidemic to some extent, but there are also some periodic rebounds, meaning the epidemic is not completely controlled, and the number of communities in the control state remains around 15.

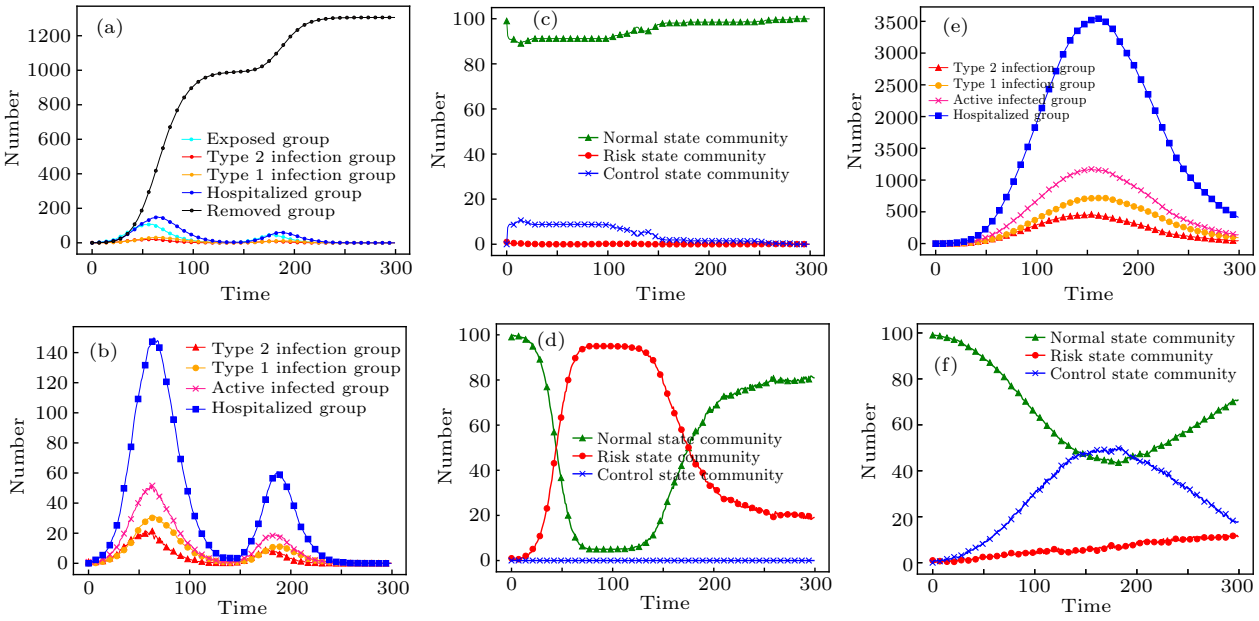


Fig. 6. Impact of community lockdown measures on epidemic spread in the community–resident dual-layer network. (a) Development trend of each resident group when community lockdown measures are adopted. (b) Development trend of each infection group when community lockdown measures are adopted. (c) Development trend of communities in different states when lockdown measures are adopted. (d) Development trend of communities in different states without lockdown measures. (e) Development trend of each resident group when no risk control measures are adopted in risk state-associated communities. (f) Development trend of communities in different states when no risk control measures are adopted in risk state-associated communities.

Due to community isolation measures, a community with diagnosed cases will transition to an isolation state, and its connected communities in the network will also shift to the isolation state. These lockdown measures effectively contain infectious residents within the community and cut off contacts between risk communities and other communities. At the same time, measures encouraging home isolation within controlled communities reduce social interaction frequencies. The adoption of community lockdown measures is equivalent to setting $\beta_c = 0$, meaning that while undiagnosed patients still exist within the community, the probability of spreading the risk to other communities is zero. The reduced social interaction frequency lowers the transmission rate β_r among residents, making the rate of susceptible residents getting infected and transitioning to the exposed state slower than the rate of exposed residents transitioning to infected states, i.e., $\beta_c k_r N_{k_r}(t)\Theta_r(t) < \gamma_{1,r} E_{k_r}(t)$. In this state, the epidemic within the community will eventually be controlled.

However, under the scenario of community lockdown measures, we also observe that the epidemic is never fully controlled, with latent cases, both types of infected cases, and diagnosed and treated cases not reduced to zero, and a second wave of the epidemic occurring. This situation arises due to two main reasons. First, the requirement for a community to transition from a control state to a normal state is the absence of newly diagnosed and treated cases within 14 days. However, among all the states of residents, only the diagnosed and treated state (H) is observable. There is a certain probability that the epidemic still exists in the form of latent cases or both types of infected cases. While the average incubation period is 5 to 7 days, there are still a few cases with much longer incubation periods, a situation that also occurs in reality.[51–53] Moreover, not all cases will transition to the diagnosed and treated state. Due to the lack of screening mechanisms, the two types of infected cases in the community remain unobservable if not diagnosed and treated. Thus, communities might lift lockdowns while still harboring risk, leading to a second wave of the epidemic. Second, the transition of a risk community to a control state is relatively delayed, occurring only after diagnosed and treated cases emerge. Although the control strategy involves transitioning all communities connected to a community with diagnosed cases to a control state, there is still a small probability that the epidemic has already spread to other community nodes beyond those connected before the diagnosed cases are identified. This delay in the discovery of diagnosed cases causes community control measures to always lag behind the epidemic's spread, preventing the epidemic from being fully controlled.

In real-world epidemic prevention and control, in addition to community lockdowns, another important measure often used is short-cycle, multiple-round, universal nucleic acid testing in risk areas. However, some views suggest that universal nucleic acid testing in risk areas has limited practical effects and low cost-effectiveness. Therefore, to verify the actual effect of this measure on epidemic control, further simulation experiments are conducted in this section.

Building on the NERCN model discussed earlier, we consider an epidemic screening mechanism for communities un-

der lockdown. During the COVID-19 pandemic, health departments in various regions implemented epidemic screening mechanisms to varying degrees in areas at risk. Nucleic acid testing in specific risk areas can actively search for potential COVID-19 infectors, aiding in further targeted measures to curb the spread of the epidemic. Hence, for communities in the control state, we define the following screening mechanisms:

When a community transitions to the control state, all residents within its jurisdiction will undergo epidemic screening.

In the control state, before returning to the normal state, all residents will undergo epidemic screening every 7 days.

During community epidemic screening, all residents in the first and second types of infection states will be identified and transitioned to the diagnosed and treated state (H), and some residents in the latent state will also be detected and transitioned to the diagnosed and treated state.

Research shows that most latent patients have a viral load in the nasopharyngeal area detectable by nucleic acid tests.[54] Therefore, we set the probability of detecting latent patients at $p = 0.5$.

Based on the description of the screening mechanism in the control state, we conduct numerical simulations of the community–resident dual-layer network model considering both community lockdown and screening mechanisms. The results are shown in Fig. 7.

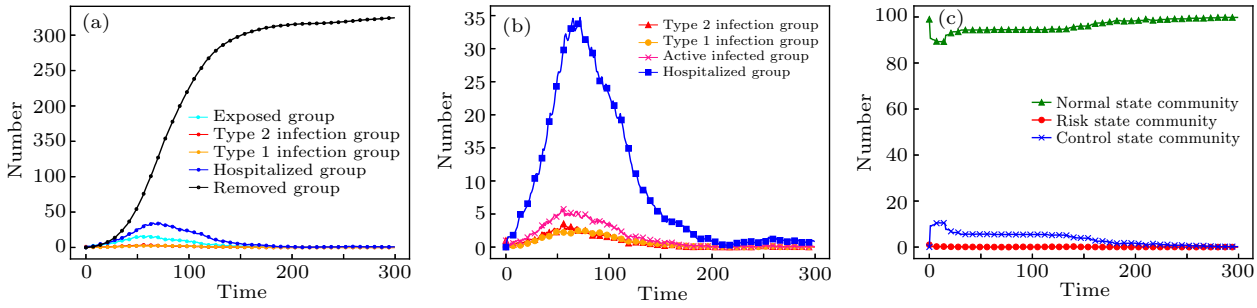


Fig. 7. Impact of community lockdown and screening measures on epidemic spread in the community–resident dual-layer network. (a) Development trend of each resident group when community lockdown and screening measures are adopted. (b) Development trend of each infection group when community lockdown and screening measures are adopted. (c) Development trend of communities in different states when lockdown and screening measures are adopted.

From Figs. 7(a)–7(c), it can be observed that after implementing risk area screening strategies in addition to community lockdown measures, the development trend of the epidemic is further controlled compared to only implementing lockdown measures (as can be seen in Figs. 6(a) and 6(c)). Specifically, the peak number of diagnosed individuals (H group) decreased from 148 to 35, with no significant change in the time it took for the epidemic to reach its peak. At the end of the simulation, the total number of residents affected by the epidemic in the lockdown and screening scenario (as shown by the black lines in Figs. 6(a) and 7(a)) decreased to 311, compared to the scenario considering only lockdown. We can conclude that when community lockdown and screening measures are implemented, the epidemic can be thoroughly controlled through proactive prevention methods. In the given system, the numbers in both types of infected groups, diagnosed and treated group, and latent state group, eventually drop to zero.

Community lockdown and screening measures compensate for the shortcomings of lockdown measures alone, i.e., the community's inability to detect residents' unobservable states, allowing latent patients to develop into both types of infected states and continue to infect susceptible individuals within the community. The lockdown and screening measures enable the community to proactively detect residents in unobservable states, allowing for the identification of hidden first and second types of infectors among residents, significantly reducing their active duration and transmission capability.

4. Conclusion and perspectives

In this paper, we establish the SE2IHR model considering two types of infected populations, based on the dynamical characteristics of major public health emergencies in real-world transmission. Further extensions are made on this basis. Firstly, the transmission dynamics of the SE2IHR model are analyzed from a network perspective. The social relationships among residents are not in the form of uniform mixing but vary, and the physical contact network of residents is generated through the Watts–Strogatz small-world network. Secondly, the dual-layer complex network structure of community–residents is considered. The community and residents form a two-layer coupled transmission network. The risk transmission at the community layer affects the epidemic transmission pattern in the resident layer, and vice versa, providing a more detailed depiction of the role of communities and residents in the epidemic transmission process. Through further numerical simulation experiments, the spread of major public health emergencies in the dual-layer complex network structure is analyzed, and various prevention and con-

trol strategies adopted by communities during the epidemic are simulated, leading to the following conclusions:

(1) Dual role of community structure in epidemic transmission: regardless of whether communities implement lockdown measures, the scale and speed of epidemic transmission are influenced by the community structure. Whether the community structure promotes or inhibits epidemic transmission depends on the degree of community aggregation. When the degree of aggregation between communities is low, the community structure serves as a barrier, slowing down the spread of the epidemic. When the degree of aggregation is high, the community structure provides connections for some long-range nodes, accelerating the spread of the epidemic. Therefore, during epidemic prevention and control, it is important to focus on the management of public areas between communities, regularly disinfect public areas in risk zones, and advocate for residents to reduce cross-community interactions. Proper lockdown measures should be taken in risk communities to prevent transferring risk to neighboring communities.

(2) Effectiveness and limitations of community lockdown measures: when there is a lack of active detection capabilities for unobservable states (latent population, hidden infectors, outlier infectors), the speed of community lockdown will always lag behind the development of the epidemic, causing a second wave. The existence of unobservable states increases the difficulty of control deployment and reduces the effectiveness of lockdowns. The health department's lack of real understanding of the epidemic situation may lead to incorrect judgments and a rebound in the epidemic, making it difficult to control completely.

(3) Efficacy of lockdown-screening strategy: nucleic acid testing provides a method to actively detect unobservable states, effectively screening the latent population and both types of infectors from the crowd. It provides necessary information support for the identification, lockdown, and unlocking of risk communities, making nucleic acid screening in risk areas a key to eliminating the epidemic. The interval between community screenings is sensitive to the effectiveness of controlling the epidemic. If the interval is too long, the situation may be similar to that of only implementing community lockdowns, i.e., the epidemic rebounds and is difficult to control completely. Therefore, in areas where the epidemic situation is more severe, the interval between screenings should be appropriately shortened.

Acknowledgements

Project supported by the Ministry of Education of China in the later stage of philosophy and social science research (Grant No. 19JHG091), the National Natural Science Foundation of China (Grant No. 72061003), the Major Program of National Social Science Fund of China (Grant No. 20&ZD155), and the Guizhou Provincial Science and Technology Projects (Grant No. [2020]4Y172).

References

[1] *COVID-19 to Plunge Global Economy into Worst Recession since World War II*
[2] Wu Y, Zhang Q, Li L, Li M and Zuo Y 2021 *Risk Management and Healthcare Policy* **2021** 4907
[3] MacQueen K M, McLellan E, Metzger D S, Kegeles S, Strauss R P, Scotti R, Blanchard L and Trotter R T 2001 *American journal of public health* **91** 1929
[4] Aldila D, Ndii M Z and Samiadji B M 2020 *Math. Biosci. Eng* **17** 6355
[5] Gilmore B, Ndejjo R, Tchetchia A, de Claro V, Mago E, Lopes C and Bhattacharyya S 2020 *BMJ global health* **5** e003188
[6] Güner H R, Hasanoğlu İ and Aktaş F 2020 *Turkish Journal of medical sciences* **50** 571
[7] Fang Y, Nie Y and Penny M 2020 *Journal of medical virology* **92** 645
[8] Wilder-Smith A, Chiew C J and Lee V J 2020 *The lancet infectious diseases* **20** e102
[9] Li M Y and Muldowney J S 1995 *Mathematical biosciences* **125** 155
[10] Annas S, Pratama M I, Rifandi M, Sanusi W and Side S 2020 *Chaos, Solitons & Fractals* **139** 110072
[11] He S, Peng Y and Sun K 2020 *Nonlinear Dynam.* **101** 1667
[12] Ferrante M, Ferraris E and Rovira C 2016 *Test* **25** 482
[13] Choi J Y 2020 *Postgraduate medical journal* **96** 399
[14] DarAssi M H, Shatnawi T A and Safi M A 2022 *Demonstratio Mathematica* **55** 265
[15] Koopman J 2004 *Annu. Rev. Public Health* **25** 303
[16] Li S L, Bjørnstad O N, Ferrari M J, Mummah R, Runge M C, Fonnesbeck C J, Tildesley M J, Probert W J and Shea K 2017 *Proc. Natl. Acad. Sci. USA* **114** 5659
[17] Niu R, Wong E W, Chan Y C, Van Wyk M A and Chen G 2020 *IEEE Access* **8** 195503
[18] Bansal S, Grenfell B T and Meyers L A 2007 *J. R. Soc. Interface* **4** 879
[19] Keeling M J and Eames K T 2005 *J. R. Soc. Interface* **2** 295
[20] Watts D J and Strogatz S H 1998 *Nature* **393** 440
[21] Hsu C I and Shih H H 2010 *Accident Analysis & Prevention* **42** 93
[22] Li J, Zhong J, Ji Y M and Yang F 2021 *Results in Physics* **25** 104283
[23] Thurner S, Klimek P and Hanel R 2020 *Proc. Natl. Acad. Sci. USA* **117** 22684
[24] Funk S, Gilad E, Watkins C, Jansen V A 2009 *Proc. Natl. Acad. Sci. USA* **106** 6872
[25] Funk S, Salathé M and Jansen V A 2010 *J. R. Soc. Interface* **7** 1247
[26] He L and Zhu L 2021 *Commun. Theor. Phys.* **73** 035002
[27] Zhao X, Zhou Q, Wang A, Zhu F, Meng Z and Zuo C 2021 *Journal of Medical Virology* **93** 4342
[28] Li D, Xie W, Han D and Sun M 2023 *Information Sciences* **651** 119723
[29] Ma W, Zhang P, Zhao X and Xue L 2022 *Physica A* **588** 126558
[30] Scabini L F, Ribas L C, Neiva M B, Junior A G, Farfan A J and Bruno O M 2021 *Physica A* **564** 125498
[31] Chung N N and Chew L Y 2021 *Scientific Reports* **11** 10122
[32] Turker M and Bingol H O 2023 *Euro. Phys. J. B* **96** 16
[33] Stegehuis C, Van Der Hofstad R and Van Leeuwaarden J S 2016 *Scientific Reports* **6** 29748
[34] Piselli F 2007 *American Behavioral Scientist* **50** 867
[35] Organization W H 2009 *Global health risks: mortality and burden of disease attributable to selected major risks* (World Health Organization)
[36] Murgante B, Balletto G, Borruso G, Las Casas G, Castiglia P and Dettori M 2020 *TeMA-Journal of Land Use, Mobility and Environment* 283
[37] Diaz P, Constantine P, Kalmbach K, Jones E and Pankavich S 2018 *Applied mathematics and computation* **324** 141
[38] Dietz K 1993 *Statistical methods in medical research* **2** 23
[39] Diekmann O, Heesterbeek J and Roberts M G 2010 *J. R. Soc. Interface* **7** 873
[40] Guerra F M, Bolotin S, Lim G, Heffernan J, Deeks S L, Li Y and Crowcroft N S 2017 *The Lancet Infectious Diseases* **17** e420

[41] Mwalili S, Kimathi M, Ojiambo V, Gathungu D and Mbogo R 2020 *BMC Research Notes* **13** 1
[42] Korobeinikov A 2004 *Mathematical medicine and biology: a journal of the IMA* **21** 75
[43] Kleinberg J M 2000 *Nature* **406** 845
[44] Ye C, Yu X and Li W 2013 *Information* **4** 398
[45] Latora V and Marchiori M 2002 *Physica A* **314** 109
[46] Xu Z and Sui D Z 2007 *Journal of Geographical Systems* **9** 189
[47] Sallaberry A, Zaidi F and Melançon G 2013 *Social Network Analysis and Mining* **3** 597
[48] Andersson C, Frenken K and Hellervik A 2006 *Environment and Planning A* **38** 1941
[49] National Health Commission of People's Republic of China http://www.nhc.gov.cn/xcs/yqtb/list_gzbd.shtml
[50] Lu J H, He J F, Zhang S X, Xie X, Wu Y S, Xu S L, Li M M and Feng T J 2021 *Practical Preventive Medicine* **28** 418
[51] Dhouib W, Maatoug J, Ayouni I, Zammit N, Ghammem R, Fredj S B and Ghannem H 2021 *Systematic Reviews* **10** 1
[52] Han Y, Jiang M, Xia D, He L, Lv X, Liao X and Meng J 2020 *Clinical Immunology* **214** 108413
[53] Wang Y, Wang Q, Wang K, Song C, Guo Z and Hu W 2021 *Infection Control & Hospital Epidemiology* **42** 242
[54] Hellewell J, Russell T W, Beale R, Kelly G, Houlihan C, Nastouli E and Kucharski A J 2021 *BMC medicine* **19** 1